

# Interfacial Properties of Nonionic Surfactants and Decane–Surfactant Microemulsions at the Silica–Water Interface. An Ellipsometry and Surface Force Study

Fredrik Tiberg<sup>\*,†</sup> and Thomas Ederth<sup>‡,‡</sup>

*Institute for Surface Chemistry, P.O. Box 5607, SE-114 86 Stockholm, Sweden, and Department of Chemistry, Surface Chemistry, Royal Institute of Technology, SE-100 44 Stockholm, Sweden*

*Received: May 24, 2000; In Final Form: July 26, 2000*

This paper features the interfacial behavior of nonionic surfactants and surfactant–decane microemulsions at the silica–water interface from micellar solutions and water-rich tricomponent  $C_nE_m$ –decane–water microemulsions. The adsorption of a nonionic surfactant (pentaethyleneglycol *n*-dodecyl ether,  $C_{12}E_5$ ) and its decane microemulsions to silica and borosilicate glass was studied by ellipsometry and direct force measurements using a bimorph surface force apparatus. The ellipsometric measurements of the adsorbed layer properties provided evidence of an initial lateral swelling of adsorbed bilayer segments with increasing bulk oil fraction. At a weight fraction of about 0.12 w/w decane-to-surfactant + decane, the surface appeared to be fully covered by a continuous bilayer with a thickness of 42 Å, a refractive index of 1.448, and an mean area per surfactant of about 49 Å<sup>2</sup>. Further increase of the oil content results in the swelling of the bilayer in the direction normal to the surface plane. Force measurements between surfactant-covered surfaces showed a subtle dependence on the properties of the glass substrate. The height of the force barrier prior to jumping into hard-wall contact was found to increase with increasing lateral surface coverage up to a decane content of 0.12 w/w. However, further increase in the fraction of decane resulted in a marked decrease of the force barrier height. The steric force onset distance, however, was always found to be proportional to the thickness of the adsorbed layers. Hence, the adsorbed layer properties measured by ellipsometry and the interaction curves measured by direct force measurements were found to correlate well. Variations were sometimes seen in force profiles measured on different glass surfaces. In most cases, the force onset distance correlated well with the thickness of two adsorbed bilayers. However, in some cases, it agreed closely with the thickness of one bilayer. These variations were not easy to predict with regard to the pretreatment and measured properties of the glass surface. Our interpretation is that this difference is caused either by very small changes in the interaction strength between adsorbed surfactant headgroups and the glass surface or by defects of the adsorbed layer resulting from the “topochemical” heterogeneity of the glass surface.

## Introduction

The importance of surfactant behavior at solid–liquid interfaces can hardly be overestimated. Much effort has consequently been directed toward acquiring a better understanding of the rather complex adsorption behavior exhibited by these molecules at solid surfaces.<sup>1–3</sup> By utilizing techniques such as neutron reflectivity,<sup>4,5</sup> ellipsometry,<sup>6,7</sup> fluorescence spectroscopy,<sup>8,9</sup> and atomic force microscopy,<sup>10–13</sup> researchers during recent years have presented a rather detailed picture of the nature of the interfacial adsorption of surfactants at different solid surfaces. A finding of relevance to this paper is the fact that nonionic surfactants self-assemble at hydrophilic surfaces to form quasi-two-dimensional analogues of the aggregate structures observed in bulk solution (cf. ref 3).

The present work concerns the characterization of interfacial properties and force interactions observed for mixed surfactant–oil systems adsorbed from dilute microemulsions (swollen micellar phase) onto silica and glass. Understanding the surface solubilization of oils and other apolar compounds is of great importance to a range of industrial processes, including deter-

gency, cleaning, flotation, and surface modification and functionalization. An improved understanding of the nature of these systems in contact with solid surfaces is also of general scientific interest. However, few fundamental studies have been performed to study multicomponent adsorption at solid surfaces.<sup>14–16</sup>

It is clear from our previous studies that ellipsometry is among the most powerful methods for in situ investigation of the interfacial behavior of surfactant systems at hard surfaces.<sup>7,17,18</sup> Not only does it provide information on fundamentally important properties such as the surface excess, the mean layer thickness, and the refractive index of the adsorbed layer, the ellipsometric technique enables the monitoring of these parameters with good time resolution, thereby also providing valuable information on the time evolution within the interfacial region during adsorption and desorption. In the current work, the emphasis was directed at equilibrium adsorbed-layer properties and their relation to interaction forces. The main aims of this work were to investigate the effects that co-adsorbed decane has on the properties of adsorbed surfactant layers and also to show how the layer properties influence the forces measured between glass surfaces covered by identical surfactant–oil systems.

Interaction forces were measured using a bimorph surface force apparatus; with this instrument, we can use macroscopic glass or silica substrates on a routine basis for force measurements.<sup>19–21</sup>

\* Corresponding author. E-mail: fredrik.tiberg@surfchem.kth.se. Fax: +46 8 208998.

<sup>†</sup> Institute for Surface Chemistry.

<sup>‡</sup> Royal Institute of Technology.

Silica and glass have been extensively used for studies of interfacial phenomena, but problems associated with the consistency of surface properties of these materials have also been reported.<sup>22,23</sup> Poor reproducibility and history dependency of the interactions in force measurements in particular are well documented.<sup>24,25</sup> These issues are also addressed in the current paper.

## Experimental Section

Pentaethyleneglycol *n*-dodecyl ether (C<sub>12</sub>E<sub>5</sub>) (Nikko Chemicals) and *n*-decane (Merck, 99%) were used as received. Water was purified with a Milli-Q purification system (Millipore). The pH was adjusted to 4 with HCl (Merck, p.a.).

The substrates for the ellipsometric measurements were oxidized silicon wafers with  $d(\text{SiO}_2) \approx 300 \text{ \AA}$ . Prior to use, these were pretreated as described in ref 6.

The instrument for the adsorption study was a modified Rudolph Research thin-film ellipsometer, type 43603-200E, equipped with high-precision stepper motors. The machine has an angle resolution of  $1/1000^\circ$ . The experimental setup and the measurement procedures are described in detail in ref 6. The technique allows simultaneous measurements of the mean thickness and refractive index (or density) with a good time resolution,  $\sim 2 \text{ s}$ . The thickness resolution during in-situ measurements of surfactant films adsorbed at silica from aqueous surfactant solutions was typically  $\pm 3 \text{ \AA}$ .<sup>7</sup>

Borosilicate glass (Pyrex) was used as the substrate for the surface force measurements. Rods 2 mm in diameter were melted in a butane oxygen burner until a spherical shape was attained at the end, the radius of which was typically 4 mm. The surfaces were mounted in the surface force instrument immediately after preparation or, where applicable, directly after post-treatment.

The bimorph surface force apparatus (MASIF, Australian Scientific Instruments) is described in detail in ref 20. One surface is mounted on a piezoelectric actuator, which in turn is mounted on a motorized translation stage providing the fine and coarse positioning of the surface. The other surface is mounted on a single cantilever spring formed by a bimorph. The bimorph is a piezoelectric device working also as a deflection sensor.<sup>26</sup> The acquisition of a force–distance profile was made in the following manner: The two surfaces were positioned at a separation distance of approximately 500 nm. They were then moved toward each other at rates between 20 and 200 nm/s. As the surfaces come into contact, they are kept together for another few hundred nanometers before being separated again; this procedure is repeated continuously. The instrument provides only indirect determination of the surface separation. Therefore, thicknesses of adsorbed layers cannot be determined by this technique unless the adsorbed layers are displaced during the approach of the two surfaces. The possibility of higher data collection rates and the ease with which, for instance, glass surfaces are prepared for use in the bimorph instrument does often favor its use in the traditional surface force apparatus (SFA, see ref 27 for the use of silica surfaces in the SFA). However, this instrument has an obvious advantage when unambiguous layer thickness values are of interest. The forces presented in the diagrams have been normalized with the harmonic mean of the radii of the surfaces.

## Results and Discussion

**Adsorbed Layer Properties.** We begin this section with a brief presentation of some central features of the interfacial behavior of nonionic surfactants adsorbed on silica to provide

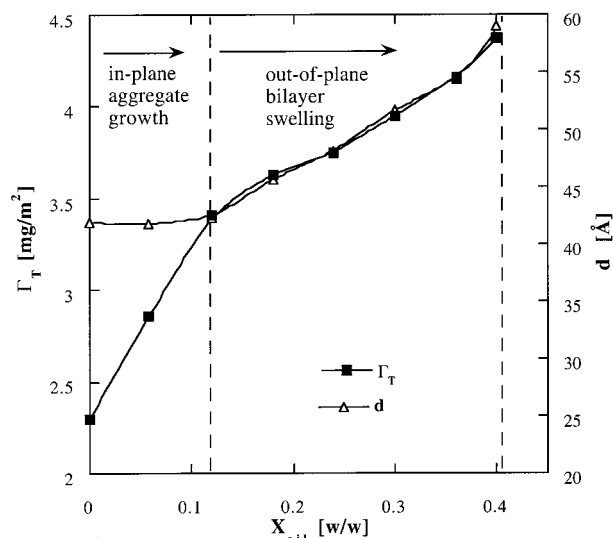


**Figure 1.** Surface excess of C<sub>12</sub>E<sub>5</sub> and decane ( $\Gamma_T$ ) and adsorbed layer thickness ( $d$ ) measured as a function of the decane-to-surfactant + decane bulk ratio by ellipsometry. The bulk concentration of surfactant + oil was always 0.1% w/w, i.e., in the region where relatively large variations of the bulk concentration have no effect on adsorption and where adsorption causes no significant change in the bulk composition.

a basis for the further discussion of the results obtained for the tricomponent (C<sub>n</sub>E<sub>m</sub>–oil–water) microemulsion systems. Non-ionic surfactants adsorb in a cooperative manner on hydrophilic surfaces such as silica. There is very little adsorption well below the critical micelle concentration (cmc). However, as the interfacial concentration exceeds a well-defined critical surface aggregation concentration (csac) below but close to the cmc, surface micellization begins, resulting in a dramatic increase of the surface excess. The density and size of adsorbed surface aggregates grow rapidly in this interval.<sup>18</sup> Plateau adsorption values are then reached at the cmc, and further changes within the interfacial region are negligible. Under these conditions, the adsorbed layer of hydrophilic surfactants such as C<sub>12</sub>E<sub>8</sub> is built up by small surface micelles, whereas more balanced surfactants such as C<sub>12</sub>E<sub>5</sub> appear to assemble into larger surface aggregates at the surface (or possibly bilayers with extensive defects, but not complete bilayers).<sup>3,13,18</sup>

In the present work, we were interested in exploring how solubilized oil affects the adsorbed layer structure and the force interactions between surfactant-covered surfaces. Figure 1 shows the evolution of adsorbed layer properties as a function of the bulk ratio of oil to surfactant (decane to C<sub>12</sub>E<sub>5</sub>). As can be clearly seen, the adsorbed amount increases with concentration in the whole interval, while the layer thickness is constant up to  $X_b = 0.12 \text{ w/w}$  and then increases in proportion to the bulk ratio of decane. The results suggest that adding decane first results in a growth of the surface aggregates in the plane of the surface. This is consistent with the fact that the solubilization of decane into the tail region of the nonionic surfactants changes the packing condition to favor flat interfaces.

A complete bilayer does seem to form at and above a decane ratio of about  $X_b = 0.12 \text{ w/w}$ . The mean refractive index of this adsorbed layer was measured to be 1.448. The refractive index increments for both the microemulsion system (at  $X_b = 0.24 \text{ w/w}$ ) and the pure C<sub>12</sub>E<sub>5</sub> system were both equal to 0.131 (perfectly linear with concentrations up to 45% w/w). Extrapolation of the refractive index increment to 100% surfactant or surfactant + oil results in a refractive index of 1.447 ( $\lambda = 4015 \text{ \AA}$  and  $n_0 = 1.340$ ), which is more or less equal to the

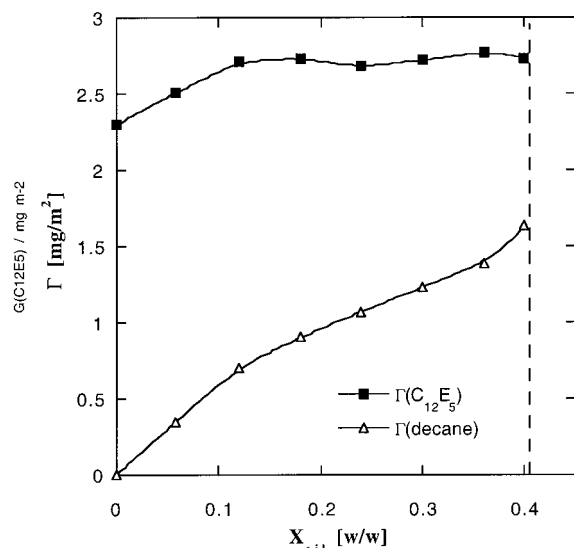


**Figure 2.** Surface excesses of  $C_{12}E_5$  and decane, respectively, measured as functions of the decane-to-surfactant + decane bulk ratio by ellipsometry. The surface excess values of the two components were calculated by using the desorption kinetics curves measured for each composition. The desorption rates of the surfactant and the oil differ by almost 2 orders of magnitude, which allows the calculation of the surface excesses of the two components separately by identifying the breakpoint in the desorption curve (see ref 15).

ellipsometric figure given above. This indicates that the adsorbed layer at  $X_b = 0.12$  w/w can be viewed as a continuous bilayer.

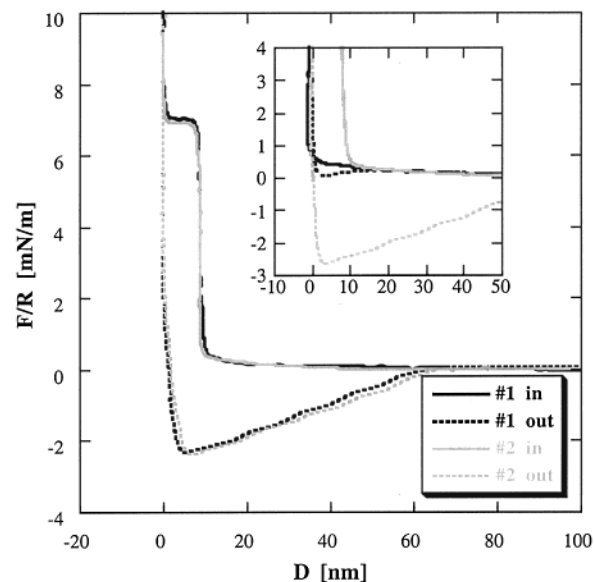
Further increase of the decane bulk ratio above 0.12 w/w results in a swelling of the bilayer in the direction normal to the surface plane. The thickness and the refractive index are in this region proportional to the decane bulk ratio.

Figure 2 shows separately the surface excess of decane and  $C_{12}E_5$  in the adsorbed layer as a function of the bulk ratio of decane. The surface excess of surfactant increases as expected until the surface is completely covered by what is assumed to be a continuous surfactant bilayer. This notion is strongly supported by the fact that the mean surface area per surfactant at the bilayer surface is  $49 \text{ \AA}^2$ , which is in good agreement with the area per  $C_{12}E_5$  molecule measured for decane-swollen  $C_{12}E_5$  monolayers ( $48 \text{ \AA}^2$ ).

We conclude that  $C_{12}E_5$  forms discrete surface aggregates or defective bilayer segments when adsorbed at the silica–water interface. When decane is added, these aggregates first grow in the plane to form a continuous bilayer at about 0.12 w/w decane-to-decane +  $C_{12}E_5$ . Further increase of the decane ratio results in an out-of-plane swelling of the bilayer. A more detailed discussion of the adsorption properties of these systems will be presented separately. From here on, we will concentrate on the relation between the adsorbed layer properties and the interaction forces.

**Interaction Forces.** Forces have been measured in neat surfactant solutions and in various surfactant + oil mixtures at a total surfactant + oil concentration of 0.1% w/w under the experimental conditions discussed above.

The forces between the surfactant-covered glass surfaces were sometimes quite unpredictable. We still cannot explain these deviating force measurements as variations in surface preparation parameters (like the flame-polishing temperature or duration, the cleaning procedure after flame polishing, the pH, the approach rate, and the equilibration time). However, most of the qualitative features of the interaction curves were discernible in all cases, indicating that the mechanisms responsible for the



**Figure 3.** Repeated force distance curves in water at pH 4 with 0.1% added  $C_{12}E_5$ . Solid lines were acquired upon approach and dashed lines upon separation. At distances beyond ca. 15 nm, the interaction is dominated by a double-layer repulsion, and as surfactant is added, steric repulsion caused by the adsorbed layers appears at a separation of 8–9 nm. The insert also shows the force–distance curve between glass surfaces measured in pure water at pH 4 (black lines).

adsorption remain the same. In this section, we start with a description of the more general behavior identified during the course of this investigation. Then we proceed to discuss the deviating data sets and possible causes of the observed mismatch.

**General Case.** Measurements between glass surfaces in water at pH 4 produce a long-range electrostatic repulsive force caused by the dissociation of surface hydroxyl groups (Figure 3). Fitting nonlinear Poisson–Boltzmann theory to the result yields a surface potential of  $-45 \text{ mV}$  and a corresponding area per charge of about  $160 \text{ nm}^2$ . The corresponding Debye screening length is about  $340 \text{ \AA}$ , which is in good agreement with the expected result for an aqueous solution set to pH  $\sim 4$ . Upon the addition of 0.1%  $C_{12}E_5$ , the repulsive force remains the same at separations exceeding 15 nm, while for shorter separations, steric repulsion caused by adsorbed surfactants is observed. The surfactant layer is expelled from the region between the surfaces at a compressive force of  $7\text{--}8 \text{ mN/m}$ , after which the two glass surfaces have presumably reached hard-wall glass–glass contact, with no, or very little, surfactant trapped between them (see Figure 3). The height of the force barrier, in an earlier study of forces between copolymer-covered hydrophobic surfaces, has been shown to be quantitatively related to the value of the surface pressure exerted by the adsorbed layers.<sup>6</sup> The adhesion between the surfaces in water is small, since the glass surface is strongly hydrated<sup>8</sup> (or it develops a surface gel in contact with water;<sup>31,33</sup> there is some controversy regarding this point). The slight adhesion-type depression in the outgoing force profile for water in Figure 3 is a hydrodynamic effect, resulting from the relatively high separation rate (equivalent to the approach rate). The pull-off force increases to approximately  $3 \text{ mN/m}$  in the presence of surfactant. This increase is probably caused by adhesive contacts of some remaining surfactant molecules in the gap between the surfaces.

Both the height and width of the steric barrier are easily reproduced as demonstrated in Figure 4, where three independent force–distance profiles are compared at different approach and separation rates. The force onset distance agrees well with

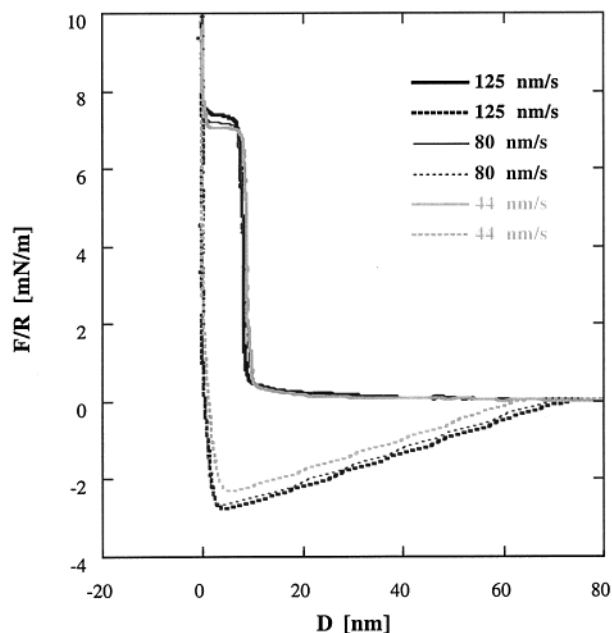


**Figure 4.** Comparison of two force–distance profiles acquired in 0.1% w/w solution of  $C_{12}E_5$  measured at different approach and separation rates. The slight shift outward in the adhesion regime as the surfaces are separated (dashed line) may be caused by the surface pressure exerted by surfactant layers outside the contact region, thus, aiding in the separation of the surfaces.

the thickness of two adsorbed bilayers (cf. Figure 1). This suggests that two of these adsorbed layers together are expelled from the contact zone when the force has exceeded about 7 mN/m, a value which is assumed to be determined by the surface pressure exerted by the adsorbed layers. The steric barrier before expulsion is very steep, which indicates that the compressibility of the adsorbed layers is quite small in this force region. In Figure 4, there seems to be a small shift of the adhesion curve outward as the surfaces are pulled apart. This may also be related to the surface pressure exerted by the adsorbed films surrounding the contact zone.

As 0.12 w/w decane is added (Figure 5) the steric repulsion remains qualitatively the same as that for the pure surfactant solution, though the distance where the steric force barrier is first observed occurs at a slightly smaller separation and the force required to displace the layer between the surfaces is higher. Adhesion forces in the presence of oil are reduced to only a few tenths of millinewtons per meter, or they have disappeared completely (Figure 5). This behavior is consistent with the surfactants in the solution with no added oil forming surface aggregates on the glass as either surface micelles or incomplete bilayers. As oil is added to the system, the adsorbate structure is changed into a dense, continuous bilayer. This is due to a change in the preferred curvature, which in turn is related to the solubilization of decane in the tail region (see Results and Discussion and Figure 2). Figure 1 shows that the mean thickness of the adsorbed layers does not change from 0 to 0.12 w/w decane-to-decane + surfactant ratio, but the force onset distance was slightly smaller for the system containing 0.12 w/w decane than for the system without decane. It is plausible that the discrete aggregates are more spherical in shape and that the maximum thickness ( $\approx$ force onset thickness) of these aggregates is slightly larger than the continuous bilayer structure in the presence of limited amounts of decane. This difference would not be detected by ellipsometry, which provides an average thickness value, whereas the force onset is representative of the absolute thickness of the adsorbed layer.

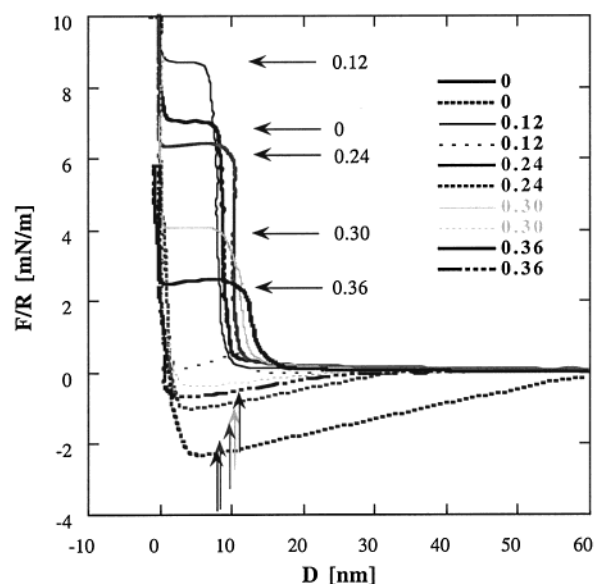


**Figure 5.** Force profiles for several surfactant + oil ratios. Solid lines are approach profiles, while dashed lines represent forces upon separation. Vertical arrows at the bottom of the figure indicate the doubled ellipsometric thicknesses from Figure 1 (increasing monotonically as the oil fraction is increased).

The higher force barrier in the presence of 0.12 w/w compared to the pure surfactant system is most likely related to an increase of the surface pressure as the adsorption increases and the structure is changed from discrete aggregates to a continuous bilayer. It is therefore not surprising that the adhesion is reduced; the increased surface pressure militates against the penetration of the layer, making glass–glass contact unfavorable. The effect of the surface pressure on the portion of the curve acquired upon the separation of the two surfaces is striking; when the surface pressure is very high, the adsorbed layer literally pushes the surfaces apart while the applied external load is still positive (Figures 4 and 5). This effect is observed for both the pure surfactant and the surfactant/oil mixtures, but its strength correlates with the expulsion force in the inward part of the force profile.

Upon further addition of oil, both the pull-off force and the force required to displace the adsorbed layer decrease monotonically. The adsorbed layers also swell when the concentration of decane increases, which is evident from Figure 5. The steric repulsion onsets are observed at separations corresponding approximately to 2 times the ellipsometric layer thickness values. These are identified with arrows in Figure 5, which shows clearly that the trend of an increasing layer thickness with increasing oil content (above 0.12 w/w decane) also is observed in force onset separations. The barrier becomes less steep with increasing oil content, and the ratio between the onset separation and the mean layer thickness seems to increase somewhat with increasing oil content. This may indicate that the outer surfactant interface, in the case of the more highly oil-swollen surface layers, is not flat but undulating (see ref 29). Such top-surface undulations may explain the increasing difference between the force onset distance and the mean layer thickness as the oil content is increased (see Figure 5). Undulations result in steric interactions at distances larger than the mean layer thickness. Figure 2 shows that while the surfactant surface excess is constant between 0.12 w/w and 0.36 w/w, the decane content increases about 3-fold.

The relation between the expulsion force and the adhesion for all investigated surfactant/oil combinations is shown in



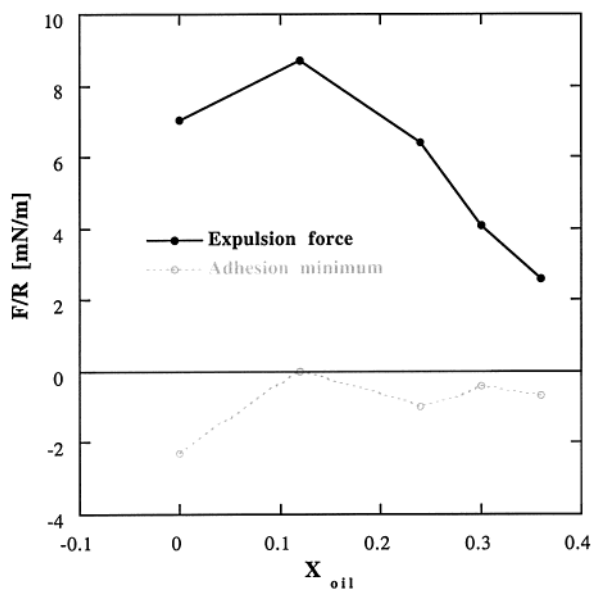


**Figure 6.** Force required to displace the surfactant layer (expulsion force) and the adhesion minima for the different investigated surfactant + oil ratios.

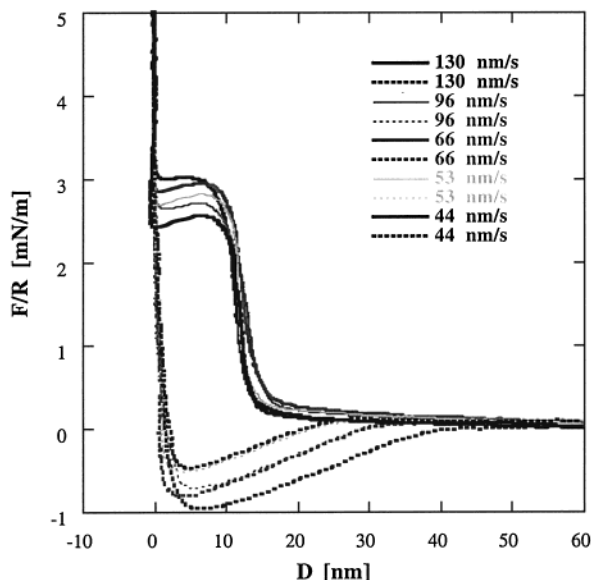


**Figure 7.** Effect of differences of the approach and separation rates for measurements at 0.36 w/w decane. The difference in the height of the barrier is to a large extent an effect of the differences in hydrodynamic forces as the approach rate is changed.

Figure 6. As stated earlier, a complete bilayer is formed at a decane ratio of 0.12 w/w, and further increase of the oil fraction results in the swelling of the bilayer in the out-of-plane direction. In this later phase, we see that the force necessary for adsorbed layer expulsion decreases with increasing oil content. We believe that this could also be related to the undulating top surface. Undulations may affect the resisting spreading pressure in the plane of the surface. A confirmation of this assumption will, however, require further theoretical work. Viscosity effects in the surface layer cannot be neglected either, and their role remains unclear; we do indeed observe a small dependence in the force curves on the rate of surface-to-surface approach at high oil fractions (see Figure 7).

The shape of the force–distance profiles is, however, not strongly rate-dependent; a small increase in the hydrodynamic repulsion caused by the drainage of the solution from the region between the surfaces is observed, as well as an accompanying

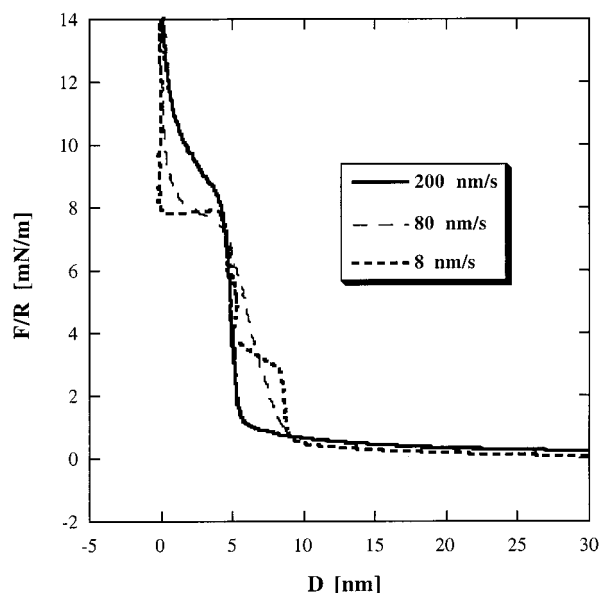


**Figure 8.** Dependence on the approach rate in a weakly adsorbing case. The steric barrier appears at a separation corresponding to the thickness of a single bilayer at the highest approach rates. As the approach rate is decreased, the onset of the steric force is moved further out, and at 8 nm/s, the displacement of two bilayers can be discerned.

increase in adhesion with increasing separation rate. The location of the steric repulsion, however, remains the same throughout. The variation in the force profiles due to the approach rate increases with increasing oil fraction.

**Anomalous Force Curves.** In our study, we occasionally observed force curves that were quite different from those discussed above. It is believed that the difference is due to small variations in the surfactant–surface interaction strength (see below) and/or the “topochemical” heterogeneity of the substrate surface. Many of the trends discussed above also hold for these measurements; the features of the interactions described in the previous section remain, though with some modifications.

The anomalous interaction force curves are similar in that the force required to displace the adsorbed layers changes with increasing oil content in a similar fashion, as discussed above. The adhesion pattern was also found to be more or less equivalent—weak or no adhesion in water, relatively strong adhesion for the pure surfactant, and a decreasing adhesion with increasing decane ratio. The major difference was manifested in the apparent force onset separation, which, in the anomalous case (see Figures 8 and 9), was seen at a separation distance about half the thickness in the earlier graphs. This could be due to the fact that the approaching surface aggregates in the anomalous case fuse or interpenetrate as the surface-to-surface contact is established. The location of the steric repulsion was indeed quite sensitive to the approach rate in this case. At very low approach rates, the steric barrier thickness stated in the previous section was indeed reproduced. This is shown in Figure 8, where the force onset is observed at double bilayer thickness for the lowest approach rate of ~8 nm/s. In contrast, the steric barrier onset for higher rates seems to correlate well with the thickness of one bilayer. Furthermore, the force barrier in the anomalous case is less distinct.

Although the force onset distances are not consistent throughout the measurements, the trend of increasing barrier height with increasing decane ratio followed by a maximum and a subsequent decrease with further increased oil fractions is well-reproduced (Figure 9). Despite efforts to systematically relate the different interaction behaviors to substrate properties (pre-

treatments, surface charge, and roughness), possible contaminants in the surfactants, and various solution properties (pH, ionic strength, and temperature), we could not discover the exact cause of the variations in the force curve character. We can only speculate that this may be due to small variations in the surfactant–surface interaction or undetectable changes in the topochemical character of the substrate surface. This points to the difficulty of interpreting the structural characteristics of adsorbed layers from force–distance curves alone. Force interactions measured by atomic force microscopy should be evaluated carefully: here, in-plane structural variations will be even more critical, and the geometry of the approaching surfaces is less well characterized. In the following discussion, we present some different substrate effects that may be the cause of the different behaviors observed in the present study.

**Substrate Effects.** Already, Rubio and Kitchener<sup>30</sup> have suggested that a combination of hydrogen bonding and hydrophobic association may be responsible for the adsorption of poly(ethylene oxide) (PEO) onto silica, an issue we addressed in a previous publication where AFM imaging and force measurements confirmed the importance of hydrophobic surfactant–surface interactions for the adsorption of nonionic surfactants at hydrophobic as well as apparently hydrophilic surfaces.<sup>31</sup> This provides further support for the view that the erratic variations in adsorption can be attributed to variations in the detailed composition of the glass surface; a difficult property to control is the ratio of silanol (hydrophilic) to siloxane (hydrophobic) groups on the surface. The former groups are known to rearrange into the latter under dehydration as the surface is heated, and the rehydration process can be very slow (see Iler<sup>22</sup>). Rubio and Kitchener reported that PEO adsorption decreased dramatically on the silica surface as a consequence of heat treatment. Dehydroxylation starts at temperatures above 700 °C but was not complete until the temperature was above 1000 °C, where PEO adsorption was effectively inhibited. In our study, neither higher temperatures (from about 1000 to 1500 °C) nor prolonged heating (10 min, as compared to the minimum requirement, approximately 10 s.) resulted in systematic changes in the observed force interaction curves. Hence, the premelting step seems not to be the primary reason for the different force interaction curves in this work. The effects of varying solution pH (to between 2 and 5), measurement temperature (15–30 °C), equilibration time (up to 24 h), and cleaning procedure (by H<sub>2</sub>O<sub>2</sub> and HCl or NH<sub>3</sub>) also did not result in significant and systematic differences in the measured steric barrier onset distance. In addition, borosilicate glass of the same kind but from two independent sources was tested, and no systematic differences were observed. We conclude that the detailed nature of the glass surfaces varies in a seemingly random manner (at least after being flame-polished). If the adsorption strength of ethylene oxide segments is very sensitive to the balance between hydrophilic and hydrophobic surface groups, it is still possible that a rather limited change in surface composition results in a marked change in the measured force interactions. Atomic force microscopy studies of glass surfaces prepared in the same manner as for the surfaces in this study show very small or no variation in roughness.<sup>32</sup> We conclude that despite extensive work, no clear cause of the occasionally measured anomalous force curves was established. For slow force measurements, however, these anomalies tend to approach the behavior seen in the normal case.

### Summary and Conclusions

The interfacial layer structure at the silica of adsorbed nonionic (C<sub>12</sub>E<sub>5</sub>) surfactants and nonionic decane–surfactant

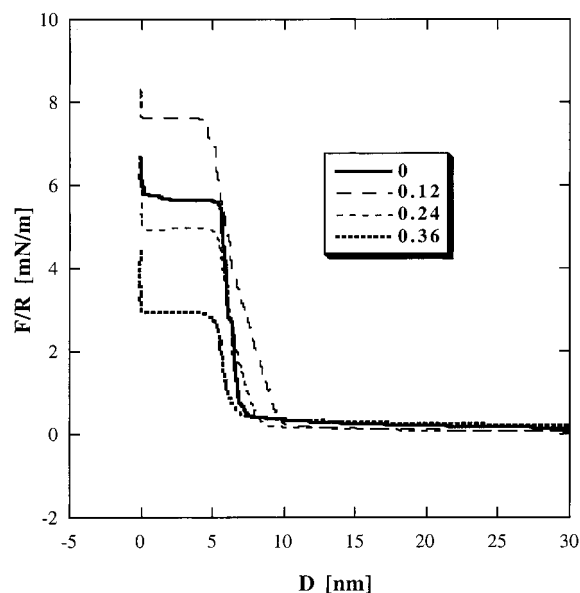


**Figure 9.** Effect of increasing oil fraction on the steric force in the anomalous case (all curves were acquired at an approach rate of 20 nm/s).

microemulsions has been studied and later related to force interactions between surfactant- and surfactant + oil-covered glass surfaces.

We show that the surfactants alone form discrete aggregates at the silica surface, a finding that agrees well with previously published literature data. Adding decane to the C<sub>12</sub>E<sub>5</sub> solution at low decane fractions (<0.12 w/w decane/decane + surfactant) results in the growth of these aggregates in the surface plane. Above 0.12 w/w, surface-solubilized decane swells the bilayers in the direction normal to the surface. In the surface-bound bilayers, the surface area per surfactant was found to be about 49 Å<sup>2</sup>, which is in excellent agreement with the measurement for the same oil-swollen surfactant aggregates in bulk solution.

The interaction force profiles show a steep steric barrier, which, at a well-defined applied load, was penetrated as the surfaces came into hard-wall contact. The force onset separation was typically slightly larger than twice the value of the corresponding layer thickness, as measured by ellipsometry. In the highly oil-swollen case, this difference increased, which was suggested to be caused by the undulation of the two outer monolayers. The force barrier decreased at high oil fractions. No firm conclusions were drawn as to the cause of this decrease. A possible explanation is that it is related to a reduction of the in-plane component of the spreading pressure of the undulating surfaces. The spreading pressure of the adsorbed films surrounding the contact area was finally further found to assist in the separation of adhering surfaces in (close to) hard-wall contact.

In our study, we also noted unpredictable variations in the measured forces with different surfaces. It was inferred that these variations were caused by inconsistencies in the chemical nature of the surfaces, causing differences in surfactant–surface interactions. This was mainly manifested in the distance at which the steric interaction was first observed. For the anomalous case, the force onset distance at higher surface-to-surface approach rates corresponded to one bilayer instead of two in the general, more ideal case. Decreasing the rate led to a recovery of the force onset at twice the bilayer thickness.

**Acknowledgment.** This work was supported by the Swedish Foundation for Strategic Research (SSF).

## References and Notes

- (1) Clunie, J. S.; Ingram, B. T. Adsorption of Nonionic Surfactants. In *Adsorption from Solution at the Solid/Liquid Interface*; Parfitt, G. D., Rochester, C. H., Eds.; Academic Press: New York, 1983; pp 105–152.
- (2) von Rybinsky, W.; Schwuger, M. J. Nonionic Surfactants: Physical Chemistry. In *Surfactant Science Series*; Schick, M. J., Ed.; Marcel Dekker: New York, 1987; Vol. 23.
- (3) Tiberg, F.; Grant, L. M.; Brinck, J. *Curr. Opin. Colloids Interface Sci.* **2000**, *4*, 411–419.
- (4) Lee, E. M.; Thomas, R. K.; Cummins, P. G.; Staples, E. J.; Penfold, J.; Rennie, A. R. *Chem. Phys. Lett.* **1989**, *162*, 196.
- (5) Lu, J. R.; Li, Z. X.; Su, T. J.; Thomas, R. K.; Penfold, J. *Langmuir* **1993**, *9*, 2408–2416.
- (6) Tiberg, F.; Landgren, M. *Langmuir* **1993**, *9*, 927–932.
- (7) Tiberg, F. *J. Chem. Soc., Faraday Trans.* **1996**, *92*, 531–538.
- (8) Levitz, P.; Van Damme, H.; Keravis, D. *J. Phys. Chem.* **1984**, *88*, 2228–2235.
- (9) Levitz, P.; Van Damme, H. *J. Phys. Chem.* **1986**, *90*, 1302.
- (10) Manne, S.; Cleveland, J. P.; Gaub, H. E.; Stucky, G. D.; Hansma, P. K. *Langmuir* **1994**, *10*, 4409–4413.
- (11) Manne, S.; Gaub, H. E. *Science* **1995**, *270*, 1480–1482.
- (12) Ducker, W. A.; Wanless, E. J. *Langmuir* **1996**, *12*, 5915–5920.
- (13) Grant, L. M.; Tiberg, F.; Ducker, W. A. *J. Phys. Chem. B*, **1998**, *102*, 4288–4294.
- (14) Harwell, J. H.; Scamehorn, J. F. Adsorption from Mixed Surfactant Systems. In *Mixed Surfactant Systems*; Ogino, K. A. M., Ed.; Marcel Dekker: New York, 1993; Vol. 46, pp 263–281.
- (15) Tiberg, F.; Brink, J. Nonionic Surfactant Systems and Surface Solubilization of Oil at the Silica–Water Interface. In *Surfactant Adsorption and Surface Solubilization*; Sharma, R., Ed.; American Chemical Society: Washington, DC, 1995; Vol. 615, pp 231–240.
- (16) Brinck, J.; Jönsson, B.; Tiberg, F. *Langmuir* **1999**, *15*, 7719–7724.
- (17) Tiberg, F.; Jönsson, B.; Lindman, B. *Langmuir* **1994**, *10*, 3714–3722.
- (18) Tiberg, F.; Jönsson, B.; Tang, J.; Lindman, B. *Langmuir* **1994**, *10*, 2294–2300.
- (19) Parker, J. L.; Rutland, M. W. *Langmuir* **1993**, *9*, 1965–1967.
- (20) Parker, J. L. *Prog. Surf. Sci.* **1994**, *47*, 205–272.
- (21) Rutland, M. W.; Parker, J. L. *Langmuir* **1994**, *10*, 1110–1121.
- (22) Iler, R. K. *The Chemistry of Silica*; John Wiley: New York, 1979; pp 644–645.
- (23) Engländer, T.; Wiegel, D.; Naji, L.; Arnold, K. *J. ColloidInterface Sci.* **1996**, *179*, 635–636.
- (24) Vigil, G.; Xu, Z.; Steinberg, S.; Israelachvili, J. *J. ColloidInterface Sci.* **1994**, *165*, 367–385.
- (25) Yaminsky, V. V.; Ninham, B. W.; Pashley, R. M. *Langmuir* **1998**, *14*, 3223–3235.
- (26) Stewart, A. M. *Meas. Sci. Technol.* **1995**, *6*, 114–123.
- (27) Horn, R. G.; Smith, D. T.; Haller, W. *Chem. Phys. Lett.* **1989**, *162*, 404–408.
- (28) Olsson, U.; Schurtenberger, P. *Langmuir* **1993**, *9*, 3389–3394.
- (29) Helfrich, W. Z. *Naturforsch.* **1973**, *28c*, 693.
- (30) Rubio, J.; Kitchener, J. A. *J. Colloid Interface Sci.* **1976**, *57*, 132–142.
- (31) Grant, L. M.; Ederth, T.; Tiberg, F. *Langmuir* **2000**, *16*, 2285–2291.
- (32) Ederth, T. Unpublished data.